International Journal of Fluid Machinery and Systems
Vol. 2, No. 2, April-June 2009

Original Paper

Numerical Analysis of the Whole Field Flow in a Centrifugal Fan for Performance Enhancement - The Effect of Boundary Layer Fences of Different Configurations

K. Vasudeva Karanth and N. Yagnesh Sharma

Department of Mechanical Engineering, Manipal University
Manipal Institute of Technology, Manipal, 576104, India

Abstract

Generally the fluid flows within the centrifugal impeller passage as a decelerating flow with an adverse pressure gradient along the stream wise path. This flow tends to be in a state of instability with flow separation zones on the suction surface and on the front shroud. Hence several experimental attempts were earlier made to assess the efficacy of using boundary layer fences to trip the flow in the regions of separation and to make the flow align itself into stream wise direction so that the losses could be minimized and overall efficiency of the diffusion process in the fan could be increased. With the development of CFD, an extensive numerical whole field analysis of the effect of boundary layer fences in discrete regions of suspected separation points is possible. But it is found from the literature that there have been no significant attempts to use this tool to explore numerically the utility of the fences on the flow field. This paper attempts to explore the effect of boundary layer fences corresponding to various geometrical configurations on the impeller as well as on the diffuser. It is shown from the analysis that the fences located on the impellers near the trailing edge on pressure side and suction side improves the static pressure recovery across the fan. Fences provided at the radial mid-span on the pressure side of the diffuser vane and near the leading edge and trailing edge of the suction side of diffuser vanes also improve the static pressure recovery across the fan.

Keywords: Boundary layer fence, Flow separation, Sliding mesh, Unsteady analysis, Recirculation zone, Jets and wakes.

1. Introduction

Flow in centrifugal impellers has always been in a state of instability with flow separation zones on the suction surface and on the front shroud. This typical flow tends itself for boundary layer separation and as a consequence, the flow field becomes distorted near the bounding surfaces of the impeller. Gallus et al. [1] have indicated a method of adopting boundary layer fences in centrifugal impellers. Sudhakar et al. [2] had extended this idea to centrifugal impellers and some encouraging results have been reported in their work. Palaniswami et al. [3] have carried out experimental study of casing treatment to improve centrifugal impeller performance. Sharma [4] investigated experimentally the effect of boundary layer fences on the exit flow in a CF Compressor.

Chung et al. [5,6,] used a boundary layer fence, inserted on the end wall of a gas turbine between two adjacent blades. It was effective in preventing the vortex from growing to its full potential strength. The fence also reduced aerodynamic losses due to secondary flow within the passage. Kawai [7] in his study has attached boundary layer fences to the blade suction surfaces and the end walls of a rectilinear turbine cascade in order to improve the aerodynamic performance of axial-flow turbines. The best combination resulted in a considerable attenuation of secondary flow, an improvement on the span wise distribution of outlet flow angles, and a large reduction in the net loss of total pressure. Rizzo [8], Canci and Rizzo [9] experimentally investigated the utility of boundary layer fences in turbine passage flow. A single boundary layer fence of varying dimensions was attached to a heated end-wall of the duct and the effect of the fence on the passage vortex was studied in a known flow configuration Results showed that the total pressure loss significantly depended on the fence dimensions. Konishi et al. [10] carried out experimental study to suppress the un-favorable flow caused due to boundary layer formation on the hub wall of a diffuser machine by applying low-height guide fences on the diffuser hub wall. Through the application of the guide fences the performance of the diffuser was improved and the optimum number of fences and the best location in the vaneless diffuser was found.

Received January 4 2009; revised March 17 2009; accepted for publication April 13 2009: Review conducted by Prof. Tong Seop Kim. (Paper number O08039)
Corresponding author: N. Yagnesh Sharma, Professor, nysharma@hotmail.com

Sullerey and Mishra [11] carried out experimental investigation to study the effect of various fences and vortex generator configurations in reducing the exit flow distortion and improving total pressure recovery in two-dimensional S-duct diffusers. The results indicated that substantial improvement in static pressure rise and flow quality is possible with judicious deployment of fences and vortex generators. Claus [12] carried out an experimental investigation of the effect of the trailing edge vortex shedding on the steady and unsteady trailing blade pressure distribution of a turbine blade at high subsonic Mach number. To limit the influence of secondary flow the blade suction sides was fitted with boundary layer fences. The oil flow visualizations showed span-wise reduction of secondary flows by 50%. Kang [13] investigated the effects of circumferential outlet distortion of a centrifugal pump diffuser on the impeller exit flow. A fence with sinusoidal width variation was installed at the vaneless diffuser exit. The flow field was measured at the impeller exit with and without the fence.

According to Fatsis et al. [14], Sorokes et al [15], Hillewaert and Van den Braembussche [16], a jet-wake (or primary and secondary) flow pattern exists at the exit of the impeller. The wake (secondary) flow position is at the suction surface or at the shroud depending on the flow rate and the impeller geometry. The flow field entering the diffuser is unsteady and distorted, and it has a significant amount of kinetic energy to transfer to the static pressure. The pressure non-uniformity caused by the volute at the off-design condition further influences the flow fields in the diffuser Shi and Tsukamoto [17] in their study have shown that the Navier-Stokes code with the k-ε model is found to be capable of predicting pressure fluctuations in the diffuser. Sofiane et al. [18] have carried out the numerical unsteady flow analysis in a vaned centrifugal fan.

A part of the work carried out in the current paper is validated with a paper by Meakhail and Park [19], which explores the study of impeller - diffuser - volute interaction in a centrifugal fan. These authors report measurement data in the region between the impeller and vaned diffuser and have obtained results of numerical flow simulation of the whole machine (impeller, vaned diffuser and volute) of a single stage centrifugal fan.

It is clear from the above literature survey that a CFD analysis on the effect of boundary layer fences on the system performance as well as its effect on Impeller-Diffuser interaction has not been explored so far. Hence a numerical modeling of the flow domain which includes a portion of the inlet to the Impeller as well as the diffuser with volute casing has been carried out and moving mesh technique [20] has been adopted for unsteady flow simulation of the centrifugal fan in this analysis.

2. Numerical Modeling

2.1 Geometry and Grid Generation

The centrifugal fan stage consists of an inlet region, an impeller, a vaned diffuser, and a volute casing (figure 1). The impeller consists of thirteen 2-D backward swept blades with an exit angle of 76^0 relative to the tangential direction. The radial gap between the impeller outlet and diffuser inlet is 15% of the impeller outlet radius. The diffuser ring has also the same number of vanes as that of the impeller. All the blades are of 5 mm thickness.

Table1. Specifications of the Centrifugal Fan

Impeller inlet radius, R_1	120 mm	Impeller inlet vane angle	30^o
Impeller outlet radius, R_2	200 mm	Impeller outlet vane angle	76^o
Diffuser inlet radius, R_3	230 mm	Diffuser inlet vane angle	23^o
Diffuser outlet radius, R_4	300 mm	Diffuser outlet vane angle	38^o
Volute Exit flange width	450 mm	Number of impeller vanes	13
Width of diffuser blade	35 mm	Number diffuser vanes	13
Width of volute casing	90 mm	Speed of the fan (RPM)	1000

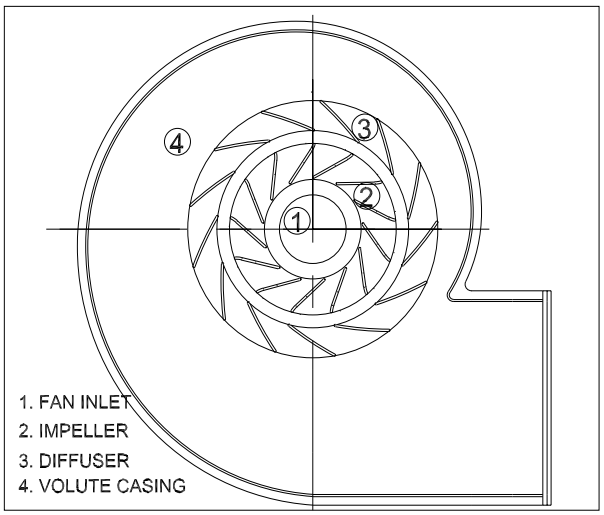

Fig. 1 Model of the centrifugal fan used in the analysis.

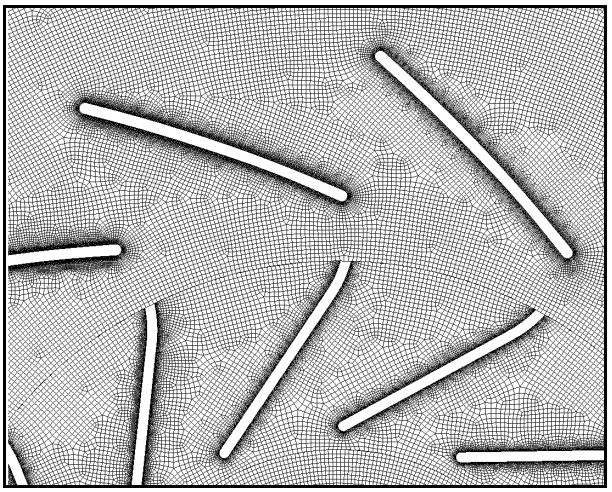

Fig. 2. A view of the meshed portion between the impeller and diffuser of the centrifugal fan

The specifications of the fan stage are illustrated in Table 1. The technical paper by Meakhail and Park [19] forms the basis for geometric modeling in the present work. Unstructured meshing technique is adopted for establishing sliding mesh configuration as the analysis is for unsteady fluctuation and is carried out using the CFD code [20].

Grid for the volute part of the domain has 163,590 nodes and 162,113 elements. The diffuser has 163,213 nodes and 155,106 elements. The impeller has 80,971 nodes and 74,143 elements. The inlet part of the domain has 5,536 and 5,190 nodes and elements respectively. The maximum size of the element is limited to elements having an edge length of 2 mm. However to establish grid independency a finer model having an element edge length of maximum of 1 mm is carried out and the variation in the results were found to be less than 2.5% and hence to save the computational time, elements edge length of maximum 2 mm size is adopted. Figure 2 shows the meshed domain and it can be observed that a finer mesh is adopted near the surface of the impeller and diffuser vanes to capture the boundary layer effects using a suitable sizing algorithm as in CFD code [20].

2.2 Unsteady Calculations Setup

Two-dimensional, unsteady Reynolds-averaged Navier- Stokes equations set to polar coordinate system are solved by the CFD code [20]. To obtain the flow characteristic curve of the fan, total pressure (gage) is applied at the inlet and static pressure (gage) is applied at the flange exit as the boundary condition. However for comparing the configurations with boundary layer fence, an absolute velocity of 5 m/s which corresponds to the design point mass flow rate of the configuration without fences is imposed at the inlet and a zero gradient outflow condition of all flow properties is applied at the flange exit of the fan, assuming fully developed flow conditions. No slip wall condition is specified for the flow at the wall boundaries of the blades, the vanes, and also the volute casing. The turbulence is simulated using a standard k-ε model [20]. Turbulence intensity of 5% and a turbulent length scale of 0.5 m which is the cube root of the domain volume are adopted in the study. The unsteady formulation used is a second order implicit velocity formulation and the solver is pressure based [20]. The pressure-velocity coupling is done using SIMPLE algorithm and discretization is carried out using the power law scheme. The interface between the impeller and the diffuser is set to sliding mesh in which the relative position between the rotor and the stator is updated with each time step. The time step Δt is set to 0.0001 s, corresponding to the advance of the impeller by $\Delta\Upsilon = 0.61^0$ per time step for a rated speed of 1000 RPM to establish stability criterion. The maximum number of iterations for each time step is set to 30 in order to reduce all maximum residuals to a value below 10^{-5}. Since the nature of flow is unsteady, it is required to carry out the numerical analysis until the transient fluctuations of the flow field become time periodic as judged by the pressure fluctuations at salient locations in the domain of the flow. In the present analysis this has been achieved after two complete rotations of the impeller. The salient locations chosen are the surfaces corresponding to, inlet to the impeller, impeller exit, diffuser exit, impeller vanes, diffuser vanes and the exit flange of the volute casing. The time and area weighted averages for the pressure and velocity fluctuations at each salient location in the computational domain are recorded corresponding to each rotation of the impeller by time step advancement. The static pressure recovery coefficient ζ_F and the total pressure loss coefficient λ_F for the diffusing domains across the fan are calculated using equation (1) and equation (2) respectively, based on the area and time weighted averages.

$$\zeta_F = \frac{1}{N}\sum_{j=1}^{j=N}\left(\frac{p_{\text{exit}} - p_2}{p_{t2} - p_2}, t_{initial} + j\Delta t\right) \quad \text{--(1)} \qquad \lambda_F = \frac{1}{N}\sum_{j=1}^{j=N}\left(\frac{p_{t2} - p_{\text{texit}}}{p_{t2} - p_2}, t_{initial} + j\Delta t\right) \quad \text{--(2)}$$

The static pressure recovery coefficient ζ_d and the total pressure loss coefficient λ_d, across the diffuser of the fan are calculated using equation (3) and equation (4) respectively.

$$\zeta_d = \frac{1}{N}\sum_{j=1}^{j=N}\left(\frac{p_4 - p_2}{p_{t2} - p_2}, t_{initial} + j\Delta t\right) \quad \text{--(3)} \qquad \lambda_d = \frac{1}{N}\sum_{j=1}^{j=N}\left(\frac{p_{t2} - p_4}{p_{t2} - p_2}, t_{initial} + j\Delta t\right) \quad \text{--(4)}$$

Where generally $p = \frac{1}{N}\sum_{j=1}^{j=N} p(area\ node, j)$

2.3 Validation of the Model

The numerical model for the whole field flow calculations is validated by calibrating the results of the current numerical work with the experimental work carried out by Meakhail and Park [19]. The graph shown in figure 3 captures the validation results for the current work with the work cited above.

The validation curve is a head coefficient versus flow coefficient curve which shows a decrease in the head coefficient as the flow coefficient increases as is required for a backward swept impeller blade. The head coefficient and flow coefficients are calculated using equation (5) and equation (6) respectively.

$$\text{Flow coefficient} \quad \phi = \left(\frac{Q}{\pi R_2^2 U_2}\right) \quad \text{- (5)} \qquad \text{Head coefficient} \quad \psi = \left(\frac{p_4 - p_1}{\rho U_2^2}\right) \quad \text{-(6)}$$

The validation shows a close agreement between the present numerical model and the experimental model of Meakhail and Park [19]

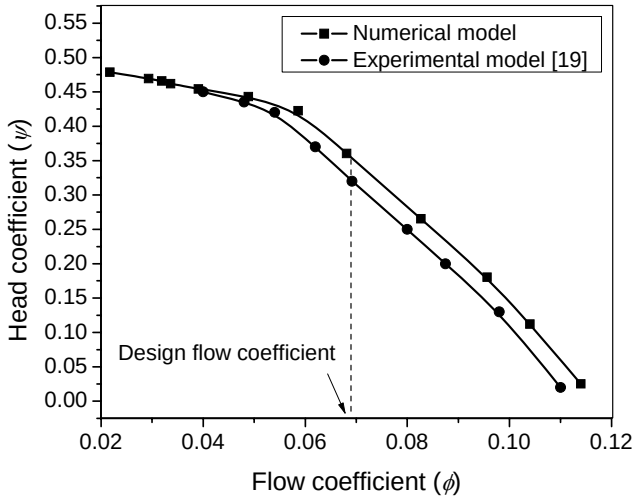

Fig. 3 Validation characteristic curve of Head coefficient vs Flow coefficient.

2.3 Geometric Modeling for Configuration with Boundary Layer Fences of the Model

A boundary layer fence is a flow re-aligning device and in the present work is chosen to be of semi-circular cross section. It is placed judiciously on the suction or pressure surfaces of impeller blades or diffuser vanes. Location of the fence is specified corresponding to the radial distance from the axis of the fan and the fence is designed to be 1 mm in height which corresponds to the local boundary layer height.

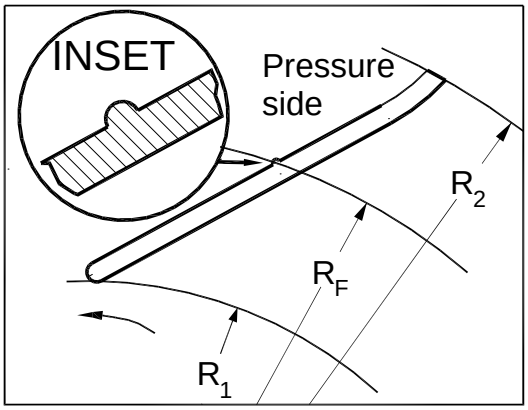

Fig.4(a) Configurations A - Boundary layer fence provided on pressure side of the impeller

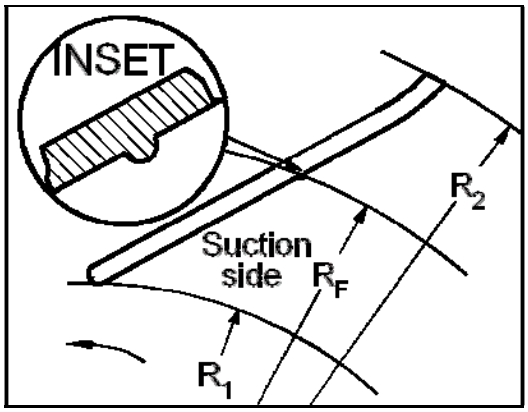

Fig. 4(b) Configurations B - Boundary layer fence provided on suction side of the impeller

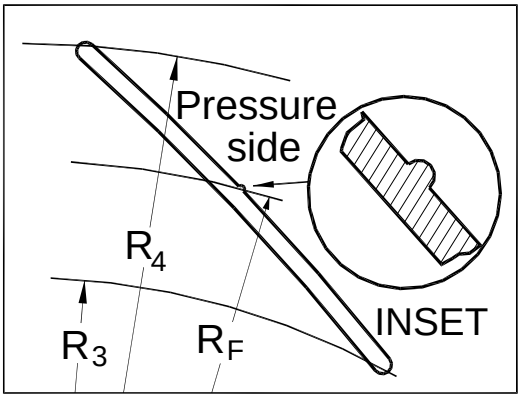

Fig. 5(a) Configurations C - Boundary layer fence provided on pressure side of the diffuser.

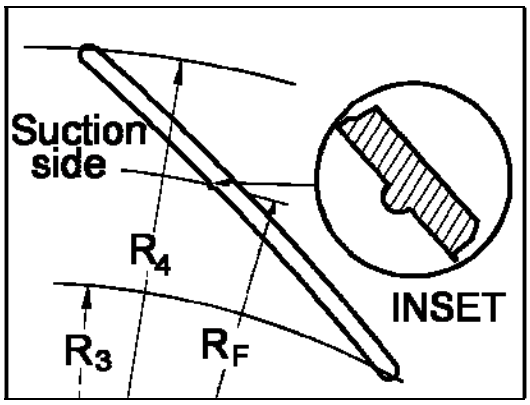

Fig. 5(b) Configurations D - Boundary layer fence provided on suction side of the diffuser

Table 2 specifies the location of the fences in terms of radial distance ratio. Configuration A and B represent the fences located on pressure side and suction side of the impeller blades respectively (fig. 4(a) and 4(b)). Configuration C and D represents the fences located on pressure side and suction side of the diffuser vanes respectively (fig. 5(a) and 5(b)). The mpeller fence radial distance

ratio R_I and Diffuser fence radial distance ratio R_d are calculated using equation 7 and equation 8 as shown below.

$$R_I = \frac{R_F - R_I}{R_2 - R_I} \quad \text{-(7)} \qquad R_D = \frac{R_F - R_3}{R_4 - R_3} \quad \text{-(8)}$$

Table 2. Radial distance ratio for configuration with fences on the impeller and diffuser.

configuration with fences on the impeller			configuration with fences on the diffuser		
Configuration type		Radial distance ratio R_I	Configuration type		Radial distance ratio R_D
Pressure side	Suction side		Pressure side	Suction side	
A1	B1	0.3	C1	D1	0.25
A2	B2	0.5	C2	D2	0.5
A3	B3	0.7	C3	D3	0.75
A4	B4	0.88	-	-	-

3. Results and Discussion

One of the methods of boundary layer control is by applying boundary layer fences on the impeller blade surfaces or diffuser vane surfaces at discrete locations. This enables the impeller or diffuser to reduce and delay the boundary layer formation. Diverting the slow-moving fluid away from the wall lets the separation regions be occupied by a faster stream of fluid, which reduces boundary-layer build-up and helps in moving the separation point to further downstream of the impeller. However since the flow patterns in each of the impeller and diffuser flow passages are different, locating the fences must be done on a trial and error basis as the flow separation point changes from one blade passage to another.

The static pressure recovery coefficient and total pressure loss coefficient for various configurations are shown in the form of bar diagrams in figures 6, 7, 11 and 12 Figures 8 to 10 and 13 to 15 shows the instantaneous velocity vector plots for various configurations.

3.1 Fence on the Pressure Side of the Impeller Blade (Configuration A)

It is seen from figure 6(a) that the overall static pressure recovery coefficient shows a significant improvement for configurations only for A4 and A2 when compared to the configuration without fence. The recovery coefficient for configuration A1 and A3 show no improvement when compared to configuration without fences. The same trend is seen in diffuser static pressure recovery coefficient as seen in figure 6(b). The above inferences agree with the total pressure loss coefficient for the same configuration types as shown in figures 7(a) and 7(b).

The physical reasoning for the above findings can be explained as follows. A large recirculation zone on the suction side of impeller blade can be seen in the relative velocity vector plots of figures 8 to 10. This causes the formation of jets and wakes near the impeller exit. A fence provided near the trailing tip of the impeller blade (configuration A4) helps to realign the jet- like flow near the pressure side and thus reduce the recirculation zone caused due to the flow separation as seen in figure 9(e). At the same time providing a fence at about 30% of the radial distance from the impeller trailing tip (configuration A3), would adversely affect the flow dynamics, since it leads to the formation of a larger recirculation zone as seen in figure 9(d). The fence provided at 50% of radial distance from the leading edge of the impeller blade (configuration A2), would enhance the flow behavior as it tends to attenuate the recirculation zones in the impeller passage figure 9(c). The fence corresponding to configuration A1 tends to re-orient the flow near the pressure side at a very early stage which causes the formation of a relatively larger recirculation zone on the impeller suction side (figure 9(b)), leading to lower static pressure recovery.

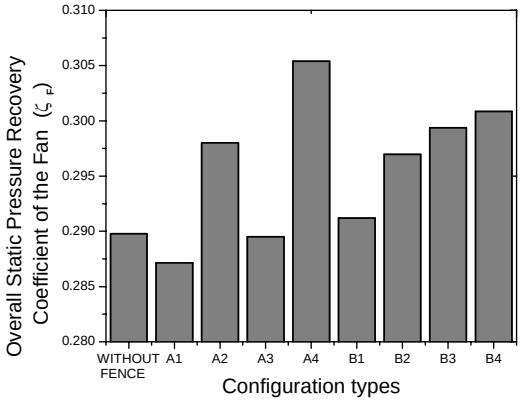

Fig. 6(a) Overall Static pressure recovery coefficient of the fan for configurations A and B.

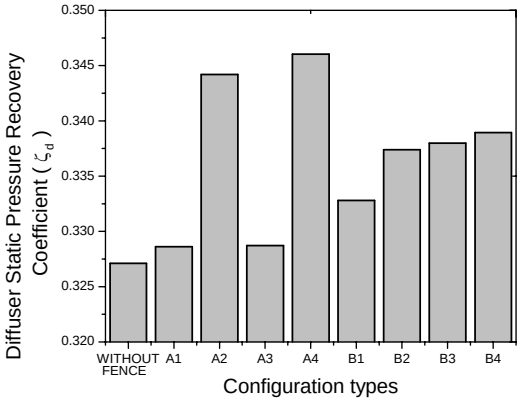

Fig. 6(b) Diffuser Static pressure recovery coefficient for configurations A and B.

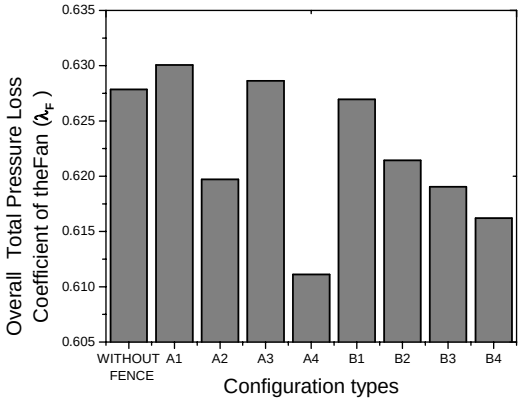

Fig. 7(a) Total pressure loss coefficient across the fan for configurations A and B.

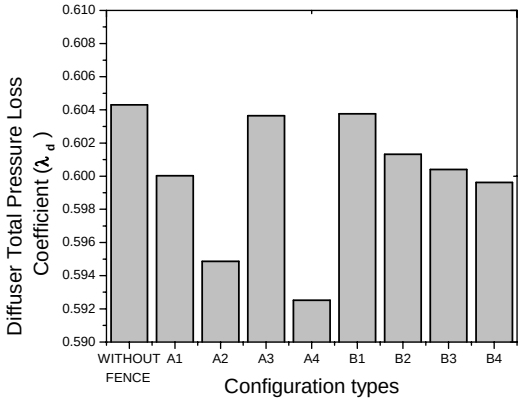

Fig. 7(b) Total pressure loss coefficient across the diffuser for configurations A and B

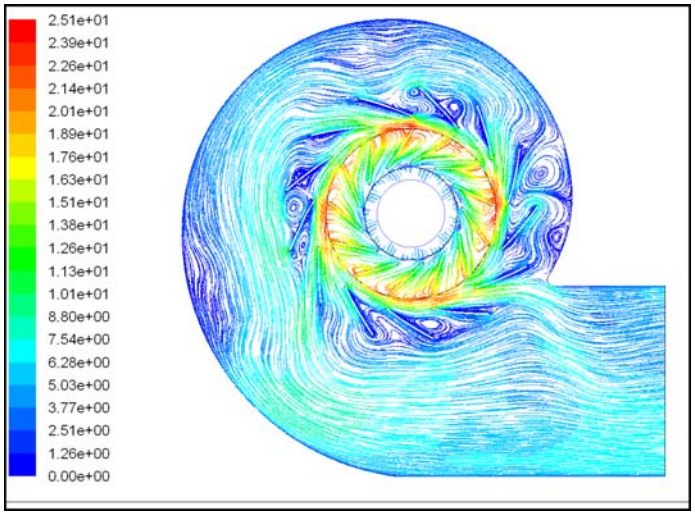

Fig. 8 Full cross sectional view of the instantaneous velocity vector plot for configuration without fence.

Hence it can be stated that the fences provided near the trailing edge or radial mid-span of the impeller pressure side, provide a better performance of the fan.

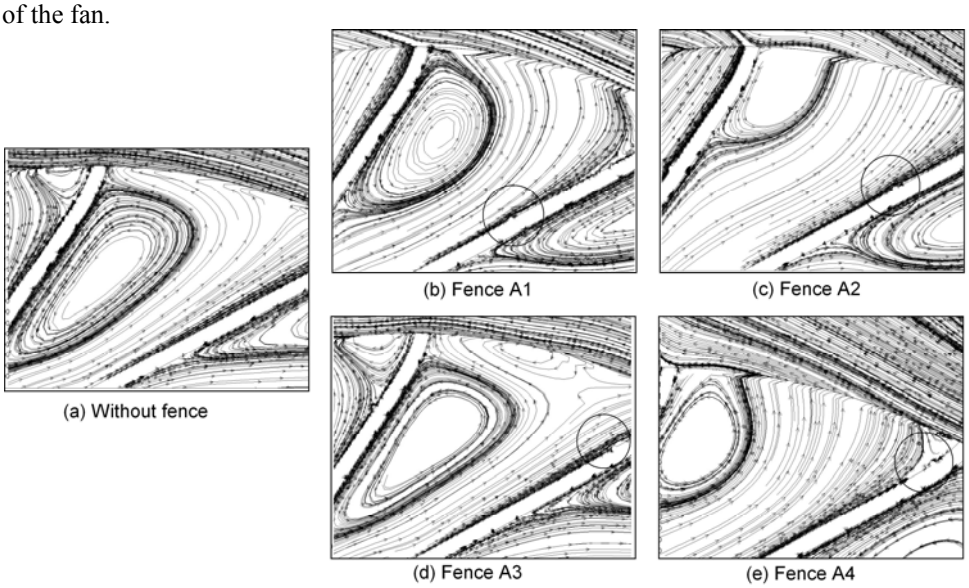

Fig. 9 Enlarged views of the velocity vector plots of flow for configuration without fence as well as for fences A1, A2, A3 and A4 on the pressure side of the impeller.

3.2 Fence on the Suction Side of the Impeller Blade (Configuration B)

It can be observed from figures 6(a) and 6(b) that the static pressure recovery coefficients for configurations B1 to B4 are better than the configuration without fence and are having an increasing trend. Configuration B4 which is near the trailing edge of the impeller blade gives the best static pressure recovery. The above observation is also supported by the declining trend of total pressure loss coefficients shown in figure 7(a) and 7(b).

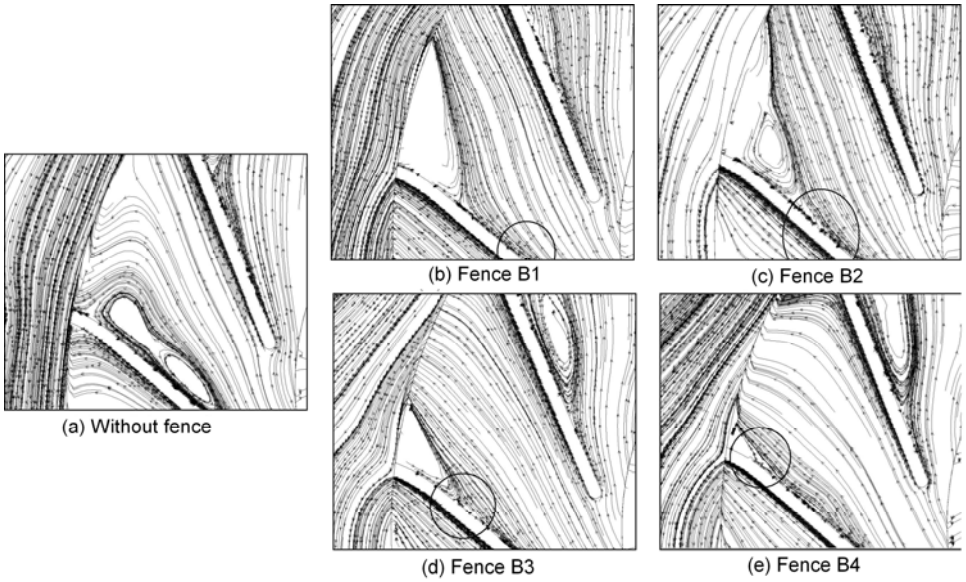

Fig. 10 Enlarged views of the velocity vector plots of flow for configuration without fence as well as for fences B1, B2, B3 and B4 on the suction side of the impeller.

The reasons for the same can be appreciated from figure 10. It can be observed in this figure that as the fence location moves up the impeller suction surface, the intensity of recirculation zone on the suction side gets reduced and hence its performance is better as an increase in static pressure recovery is achieved. It can be also noted that the fence near the trailing tip of the impeller suction side (configuration B4) enables the impeller to block the formation of recirculation zone at a very early stage (figure 10 (e)) and this ensures through flow in the impeller leading to better performance.

Hence it can be positively stated that the fence provided on the suction side of the impeller improves the static pressure recovery of the fan and the most suitable location would be near the trailing edge of the impeller blade.

3.3 Fence on the Pressure Side of the Diffuser Vane (Configuration C)

Figures 11(a) and 11(b) show the static pressure recovery coefficient for configuration C with fences located on the pressure side of diffuser vanes. Figures 13 and 14 show the instantaneous velocity vector plots for configurations C1, C2 and C3 respectively.

It can be noted that the fence provided on the pressure side at the radial mid span of diffuser vanes (configuration C2) develops an improved static pressure recovery and fences with configurations C1 and C3 would adversely affect the static pressure recovery. The reasoning for this effect can be explained with the help of figure 13(b) in which it can be clearly observed that a fence provided near the leading edge of the diffuser tends to decelerate the flow on the stationary vanes and this causes flow separation leading to the formation of a large recirculation zone in some of the flow passages. However a fence near the radial mid span (configuration C2) helps in neutralizing aforementioned recirculation zones (figure 13(c)) which in turn yield a better static pressure recovery. Further, the fence near the trailing edge of the vane (configuration C3), tends to move the recirculation zone toward the upstream as shown in figure 13(d) which leads to lower static pressure recovery. In another diffuser flow passage the fence C3tends to draw the recirculation zone towards it which causes enlargement of the recirculation zone (figure 14(b)) which helps in tripping the flow causing deceleration of the flow. This is reflected in figures 12(a) and 12(b) which show a greater total pressure loss coefficient for configuration C3.

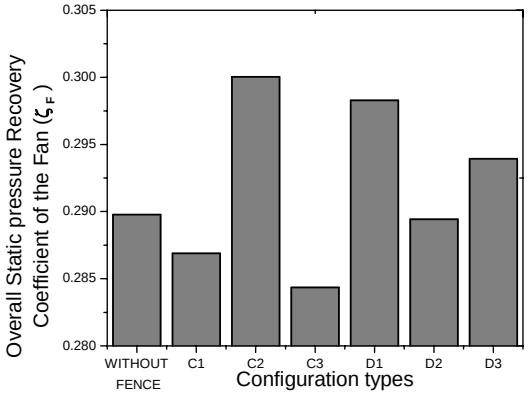

Fig. 11(a) Overall Static pressure recovery coefficient of the fan for configurations C and D

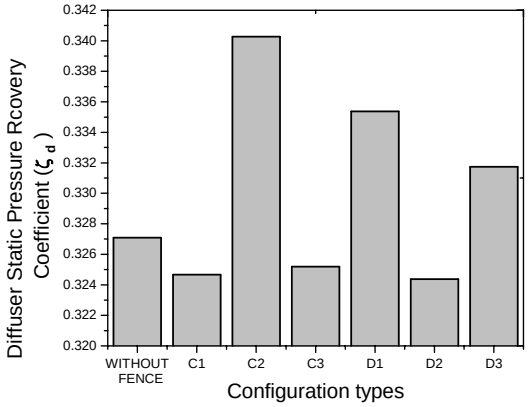

Fig. 11(b) Diffuser Static pressure recovery coefficient for configurations C and D.

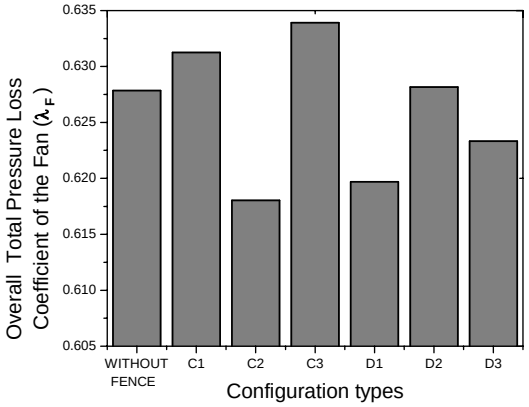

Fig. 12(a) Total pressure loss coefficient across the fan for configurations C and D.

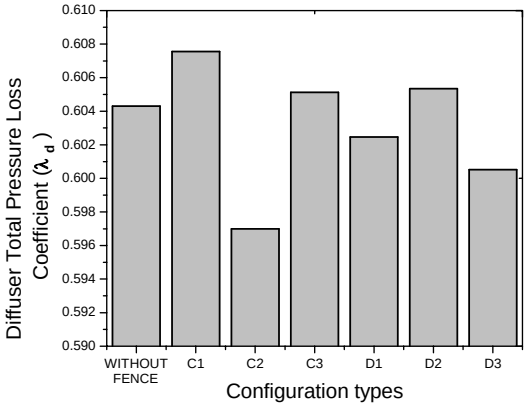

Fig. 12(b) Total pressure loss coefficient across the diffuser for configurations C and D.

Hence it can be stated that fences provided at the radial mid span of the pressure side of the diffuser tends to improve the static pressure recovery of the fan and fences provided near the trailing or leading edge of the diffuser vanes would adversely affect the static pressure recovery of the fan.

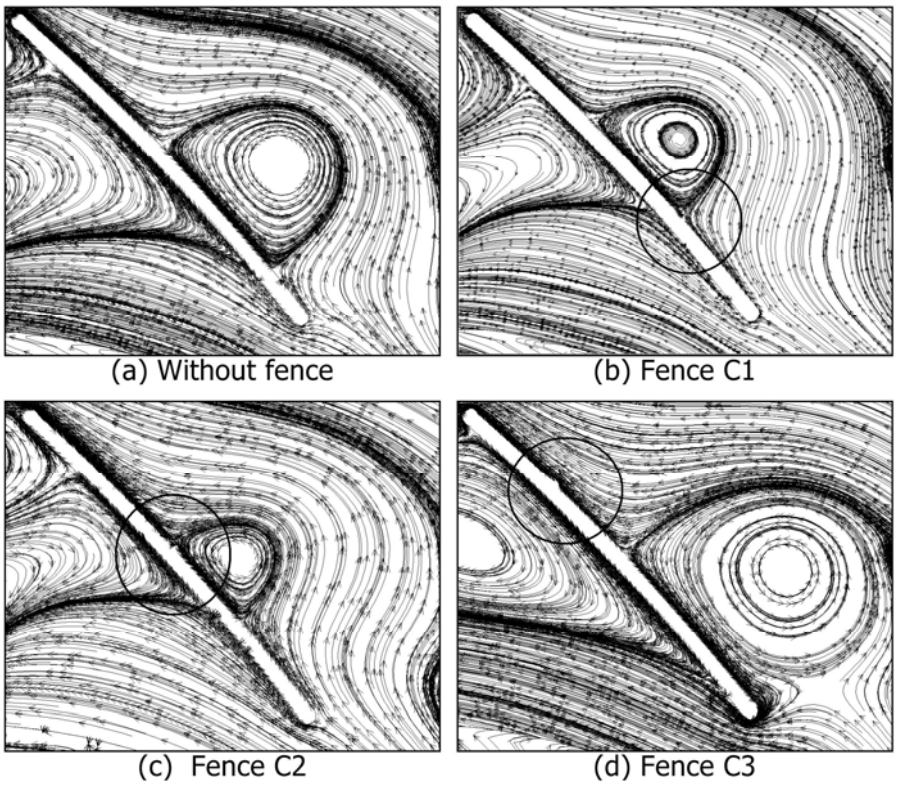

Fig. 13 Enlarged view of the velocity vector plots of flow in configuration without fence as well as for configurations C1, C2 andC3 on the pressure side of the diffuser.

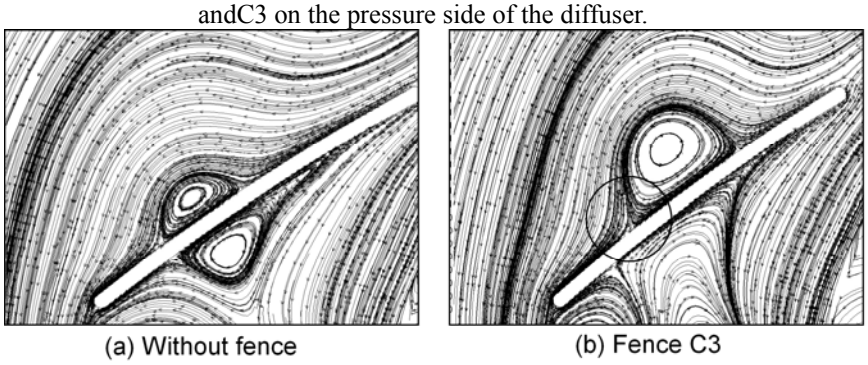

Fig. 14 Enlarged vector plots for configuration without fence and configurations C3

3.4 Fence on the Suction Side of the Diffuser Vane (Configuration D)

Figures 11(a) and 11(b) show the static pressure recovery coefficient for configuration D with fences located on the suction side of the diffuser vanes.

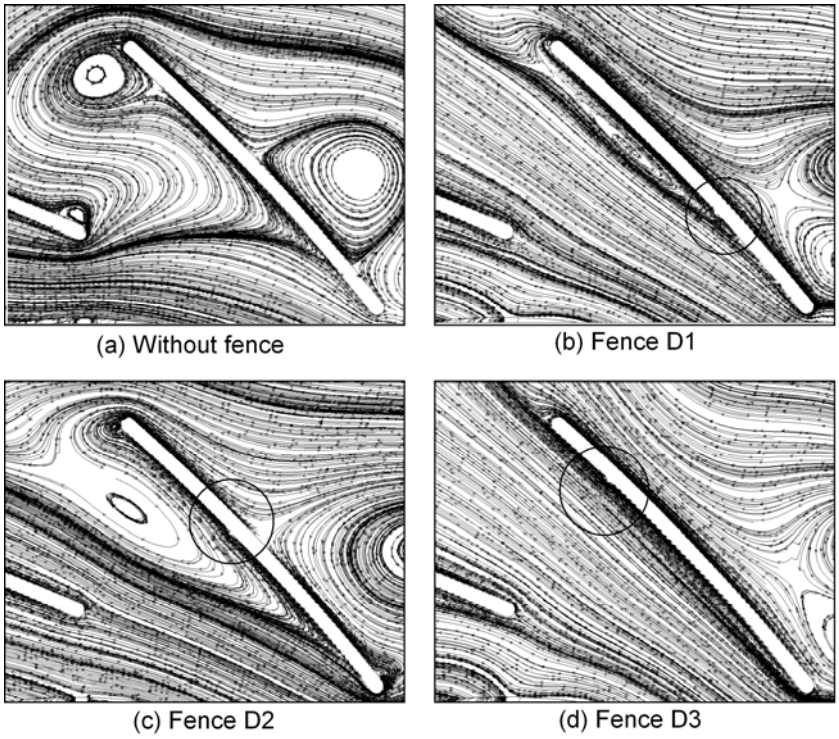

Fig. 15 Enlarged views of the velocity vector plots of flow for configuration without fence as well as for fences D1, D2, and B3 on the suction side of the diffuser.

It is noted that the fences provided on the suction side of the diffuser vane improves the static pressure recovery of the fan when compared with the configuration without fence. However the fence provided near the leading edge of the diffuser vane (configuration D1) gives relatively higher static pressure recovery and fence provided at the radial mid span of the vane (configuration D2) gives relatively lower recovery when compared to configuration without fence. The fence for configuration D3 (which is near the trailing edge of the diffuser vane) also shows a slight improvement in the static pressure recovery when compared to configuration without fence.

Physically the above noted phenomena that, generally the fences provided on the suction side seem to improve static pressure recovery (Fig. 15) could be attributed to the fact that the presence of the fence greatly aids in reorienting the flow from a possible stalled condition (Fig.15(a)). The better fluid guidance in the vane passages is clearly visible in Fig. 15 (b) due to the fence configuration D1. Similar is the case for configuration D3. However configuration D2 only helps achieving eliminating the stall but still leaving a large trailing edge vortex in the downstream direction.

The above observations are corroborated by the lower total pressure recovery coefficients as shown in figures 12(a) and 12(b).

4. Conclusion

The following conclusions can be drawn from the above analysis.

a. Boundary layer fences provided on impeller blades and diffuser vanes at suitable locations tend to improve the performance of the centrifugal fan, in terms of higher static pressure recovery coefficients and reduced total pressure loss coefficients.

b. Boundary layer fence provided near the trailing edge of the impeller pressure side and suction side improves the performance of the fan. (Configuration A4 and B4)

c. Boundary layer fence provided at the radial mid span of the diffuser vane pressure side tends to improve the performance (configuration C2) and fences near the leading edge and trailing edge of the pressure side of the vane would tend to adversely affect the performance. (Configuration C1 and C3)

d. Boundary layer fence near the trailing and leading edge of the suction side of the diffuser vanes (configurations D1 and D3) would improve the performance of the fan and relatively higher recovery is possible when the fence is located near the leading edge of diffuser suction side (Configuration D1).

Acknowledgments

The authors wish to acknowledge and thank Tarek Meakhail and Seung O Park [19], for readily giving the centrifugal fan drawing for their numerical modeling. They also wish to thank Manipal Institute of Technology, Manipal University, for providing computational resources for undertaking this study.

Nomenclature

p_i	Static pressure (Pa) (i = 1,2,3,4)	γ	The angle of advance of a given impeller blade to its next adjacent blade position.
p_{ti}	Total pressure (Pa) (i = 1,2,3,4)		
i	*1* = impeller inlet,, *2* = impeller exit,, *3* = diffuser inlet, *4* = diffuser exit	ϕ	Flow coefficient
		ψ	Head coefficient
p_{exit}	Static pressure at flange exit (Pa)	ζ_F	Overall static pressure recovery coefficient of the fan
$p_{t\,exit}$	Total pressure at flange exit (Pa)	λ_F	Overall total pressure loss coefficient across the fan
U_2	Tangential velocity at impeller exit (m/s)	ζ_d	Static pressure recovery coefficient across the diffuser
ρ	Air density (Kg/m^3)	λ_d	Total pressure loss coefficient across the diffuser ,
Q	Volume flow rate per unit channel height		
		j	General parameter,
R_F	Radius at which fence is located	N	General parameter
R_I	Impeller fence radial distance ratio	t	Time step size in s
R_D	Diffuser fence radial distance ratio		

References

[1] Gallus, H.E. and Subramanian, S., 1978, "Experimental investigation in centrifugal impellers," First International Conference on Centrifugal Compressor Technology, I. I. T. Madras, India.

[2] Sudhakar, C.V., Palaniswami, P.N. and Gopalakrishnan, G., 1978, "Boundary Layer Fences in Radial Compressor - a Preliminary Report," Eighth National Conference on Fluid Mechanics and Fluid Power, Coimbatore, India.

[3] Palaniswami, P.N., Gopalakrishnan, G. and Prithviraj, D., 1979, "Boundary Layer Fences and Casing Treatment to Improve Centrifugal Impeller Performance," Ninth National Conference on Fluid Mechanics and Fluid Power, SVRCET, India.

[4] Sharma, N.Y., 1981, "Investigation of Boundary layer Fences on the Exit Flow Characteristics in a Centrifugal Compressor Impeller," M.Tech Dissertation, IIT, Madras, India.

[5] Chung, J.T., Simon, T.W., and Buddhavarapu, J., 1991, "Three-Dimensional Flow Near the Blade/Endwall Junction of a Gas Turbine: Application of a Boundary Layer Fence," ASME Paper No. 91-GT-45.

[6] Chung, J.T., and Simon, T.W., 1993, "Effectiveness of the Gas Turbine Endwall Fences in Secondary Flow Control at Elevated Free stream Turbulence Levels," ASME Paper No. 93-GT-51.

[7] Kawai, T., 1994, "Effect of Combined Boundary Layer Fences on Turbine Secondary Flow and Losses," JSME international journal. Series B, Fluids and Thermal Engineering, vol. 37, no. 2, pp. 377-384.

[8] Rizzo, D.H., 1994, "The Aerodynamic and Heat Transfer Effects of an Endwall Boundary Layer Fence in a 90 Degree Turning Square Duct," M.S. Thesis Pennsylvania State Univ., University Park, PA. Dept. of Aerospace Engineering, United States.

[9] Cengiz C. and Rizzo, D.H., 2002, "Secondary Flow and Forced Convection Heat Transfer Near Endwall Boundary Layer Fences In a 90 degree Turning Duct," International Journal of Heat and Mass Transfer, 45. pp. 831-843.

[10] Konishi, T., Sakai, T. and Whitfield, A., 1998, "Performance Improvement of a Mixed-Flow Fan Through the Application of Guide Fences in the Vaneless Diffuser," Proceedings of the Institution of Mechanical Engineers, Part- A: Journal of Power and] Energy, Professional Engineering Publishingy, Volume 212, No. 4, pp. 217-224.

[11] Sullerey, R.K. and Mishra, S., 2002 "Application of Boundary Layer Fences and Vortex Generators in Improving Performance of S-Duct Diffusers," ASME Journal of Fluids Engineering , 3, 124, Issue 1, pp. 136-142.

[12] Claus, H.S., 2003, "Turbine Blade Trailing Edge Flow Characteristics at High Subsonic Outlet Mach Number," ASME J. Turbomachinery., April, Volume 125, Issue 2. pp. 298-309.

[13] Kang, S., 2004, "Flow at the Centrifugal Pump Impeller Exit With Circumferential Distortion of the Outlet Static Pressure," ASME J. Fluids Eng. January , Volume 126, Issue 1, pp. 81-87

[14] Fatsis, A., Pierret, S. and Van den Braembussche, R., 1997, "Three-dimensional unsteady flow and forces in centrifugal impellers with circumferential distortion of the outlet static pressure," Journal of Turbomachinery, 119, pp 94-102.

[15] Sorokes, J. M., Borer, J.C. and Koch, J.M., 1998, "Investigation of the circumferential static pressure non-uniformity caused by centrifugal compressor discharge volute," 98 GT 326, International Gas Turbine & Aeroengine Congress & Exhibition, Stockholm, Sweden.

[16] Hillewaert, K. and Van den Braembussche, R.A., 1999, "Numerical simulation of impeller-volute interaction in centrifugal compressors," Journal of Turbomachinery, 121, pp 603-608.

[17] Shi, F. and Tsukamoto, H., 2001, "Numerical Study of Pressure Fluctuations Caused by Impeller-Diffuser Interaction in a Diffuser Pump Stage," Transactions of the ASME, 9, Vol. 123, pp. 466-474.

[18] Sofiane, K., Smaïne, K., Farid, B. and Robert, R., 2005, “Flow Study in the Impeller-Diffuser Interface of a Vaned Centrifugal Fan,” ASME J. Fluid Engineering, 5, vol. 127, pp. 495-502.
[19] Meakhail, T. and Park, S.O., 2005, “A Study of Impeller-Diffuser-Volute Interaction in a Centrifugal Fan,” ASME Journal Turbomachinery, 127, pp. 84-90.
[20] Fluent 6.3, Fluent Inc., 2006.